Journal of Alloys and Compounds 729 (2017) 988–991

Contents lists available at ScienceDirect

Journal of Alloys and Compounds

journal homepage: http://www.elsevier.com/locate/jalcom

Gd substitution for Ce in preparing (Ce,Gd)-Fe-B magnets

Zhu-bai Li [a, c, *], Dong-shan Wang [a, b], Zhi-xin Zhang [a, b], Xue-feng Zhang [a, b], Feng-xia Hu [c], Ji-rong Sun [c], Bao-gen Shen [c]

[a] Key Laboratory of Integrated Exploitation of Bayan Obo Multi-Metal Resources, Inner Mongolia University of Science and Technology, Baotou 014010, China
[b] School of Science, Inner Mongolia University of Science and Technology, Baotou 014010, China
[c] State Key Laboratory for Magnetism, Institute of Physics, Chinese Academy of Sciences, Beijing 100190, China

ARTICLE INFO

Article history:
Received 24 April 2017
Received in revised form
29 July 2017
Accepted 22 September 2017
Available online 23 September 2017

Keywords:
Rare-earth alloys
Ce-Fe-B magnets
Gd
Coercivity

ABSTRACT

Ce-Fe-B rare-earth alloys are alternative to substitute partially for Nd-Fe-B permanent magnets for reducing the cost and the balance use of rare-earth elements. However, coercivity is rather low in Ce-Fe-B magnets, which partially ascribes to the instability of $Ce_2Fe_{14}B$ phase and the low magnetocrystalline anisotropy. In this paper, magnetic properties are investigated in $Ce_{13-x}Gd_xFe_{81}B_6$ ribbons via substituting of Gd for Ce. X-ray diffraction shows that a little amount of Gd substitution for Ce leads to an increase in the intensity of diffraction peak for main phase, which should be attributed to the improvement of the stability of $R_2Fe_{14}B$ phase and the reduction in the amount of amorphous phase. Even though the magnetocrystalline anisotropy is lower in $Gd_2Fe_{14}B$ than that in $Ce_2Fe_{14}B$, the coercivity increases to 5.88 kOe for a little amount of Gd substitution in $Ce_{12}Gd_1Fe_{81}B_6$ ribbons. For Gd atomic percent more than 3% the coercivity decreases, and the remanence drops significantly. With the increase of Gd atomic percent, Curie temperature increases monotonically. Henkel plots indicate that Gd substitution for Ce could enhance the effect of exchange coupling, which owes to the increase of exchange coefficient in main phase as well as to the reduction in the amount of amorphous phase. These investigations show that a little amount substitution of Gd is beneficial to improve the magnetic properties without a significant drop of the remanence.

1. Introduction

Ce-based rare-earth alloys have attracted many attentions owing to the abundance and low cost of Ce element in rare-earth resource [1–8]. $Ce_2Fe_{14}B$ alloy bears the magnetocrystalline anisotropy of 26 kOe [9], theoretically, which could be used as low cost permanent magnets with moderate magnetic properties and may partially substitute for $Nd_2Fe_{14}B$ magnets for the balance use of rare-earth elements [10–16]. However, the phase diagram and phase constitution of Ce-Fe-B ternary alloys are different from those of Nd-Fe-B [17,18], and the coercivity is rather low in Ce-Fe-B magnets [19]. Besides $Ce_2Fe_{14}B$ main phase, there exist minor phases of $CeFe_2$, $CeFe_7$ and Fe_3B in Ce-Fe-B ribbons [19], and the amount of minor phases is larger in Ce-Fe-B ternary alloy compared with the corresponding Nd-Fe-B alloy [19]. The minor phase is soft magnetic phase or paramagnetic phase, which would decrease coercivity and deteriorate the squareness of demagnetization curve. Optimizing the content of Ce in Ce-Fe-B ternary alloy could suppress the formation of minor phases $CeFe_7$ and Fe_3B, and the amount of minor phase is reduced for Ce atomic percent of 13% in $Ce_{13}Fe_{81}B_6$ ribbons [19]. It also reported that the heavy rare-earth element Ho could optimize the microstructure of R-Fe-B alloys [20]. However, Ho is scarce in rare-earth resource and expensive. Gd is the heavy rare-earth element but inexpensive. In this paper, we prepared $(Ce,Gd)_{13}Fe_{81}B_6$ ribbons and investigated the effect of Gd substitution on the phase constitution and magnetic properties, which is expected to serve as reference for the composition design on the resource-saving Ce-based rare-earth magnets.

2. Experimental

High purity Ce, Gd, Fe, and Fe-B alloy were mixed according to the nominal composition of $Ce_{13-x}Gd_xFe_{81}B_6$ (x = 0, 0.2, 0.5, 0.8, 1, 3,

* Corresponding author. Key Laboratory of Integrated Exploitation of Bayan Obo Multi-Metal Resources, Inner Mongolia University of Science and Technology, Baotou 014010, China.
E-mail address: lzbgj@163.com (Z.-b. Li).

https://doi.org/10.1016/j.jallcom.2017.09.243
0925-8388/

5, 8, 11, and 13). The precursor ingot was obtained via melting the mixture by arc-melting technique under an argon atmosphere. For ensuring composition homogeneity each ingot was re-melted at least three times. Crushed the ingot into small pieces and inserted them into a quartz tube, the diameter of whose bottom orifice is in the range of 0.8–1.0 mm. The small pieces of ingot were melted by induction melting in the chamber filled with high purity argon, and then the melt was ejected through the orifice onto the surface of a rotating copper wheel by pressured argon. The surface of copper wheel was polished by the 1000-grit paper, and the surface velocity was set in the range of 25–27 m/sec for optimizing the coercivity and the squareness of demagnetization curve. The phase constitution of the ribbons was examined by x-ray diffraction (XRD) using Co Kα radiation. Magnetic measurements were performed using Quantum Design Versalab at temperature of 300 K, and the field direction is in the plane of the ribbons and therefore the demagnetization factor was neglected.

3. Results and discussion

Fig. 1 shows the hysteresis loops for the optimally melt-spun ribbons. The variation of coercivity with Gd content is shown in the inset of Fig. 1. The coercivity is 4.43 kOe in $Ce_{13}Fe_{81}B_6$ alloy. A little amount substitution of Gd for Ce leads to an increase of coercivity, which reaches to 5.88 kOe in $Ce_{12}Gd_1Fe_{81}B_6$ ribbons, but the coercivity decreases for Gd atomic percent larger than 3%. The substitution of Gd for Ce results in the monotonous decrease of the remanence, which should be due to the low value of saturation magnetization in $Gd_2Fe_{14}B$ [9].

High coercivity originates from the uniaxial magnetocrystalline anisotropy in rare-earth $R_2Fe_{14}B$ magnets, and the magnetocrystalline anisotropy of $Gd_2Fe_{14}B$ is lower than that of $Ce_2Fe_{14}B$ [9]. However, as shown in Fig. 1, a little amount substitution of Gd leads to an increase of coercivity. Besides the magnetocrystalline anisotropy, the microstructure has strong effect on the coercivity. For making it clear about the microstructure, the phase constitution and grain size were checked by the x-ray diffraction (XRD). Fig. 2 shows the XRD patterns for $Ce_{13}Fe_{81}B_6$, $Ce_{12.8}Gd_{0.2}Fe_{81}B_6$, $Ce_{12}Gd_1Fe_{81}B_6$, $Ce_8Gd_5Fe_{81}B_6$, and $Gd_{13}Fe_{81}B_6$ ribbons. The average grain sizes are estimated to be in the range of 20–30 nm using Jade software. Most of diffraction peaks correspond to $R_2Fe_{14}B$ phase, confirming the main phase of $R_2Fe_{14}B$ in these ribbons. However, the diffraction peaks are much weaker for $Ce_{13}Fe_{81}B_6$ ribbons, indicating that there coexists amorphous phase in these ribbons [21]. This fact implies the difficulty in the crystallization of $Ce_2Fe_{14}B$ phase even for the optimization of chemical composition in ternary Ce-Fe-B ribbons [19], which may be related with the difference of

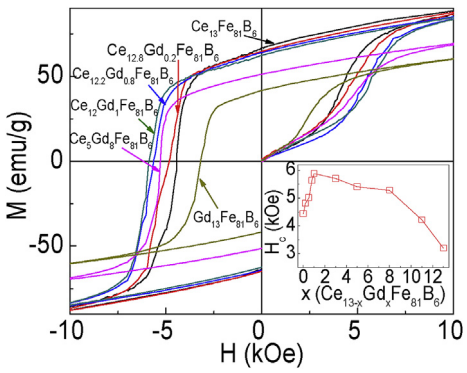

Fig. 1. The hysteresis loops for (Ce,Gd)-Fe-B ribbons at temperature of 300 K, and the inset shows the dependence of coercivity on the Gd atomic percent.

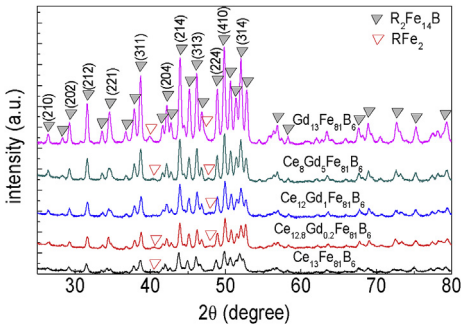

Fig. 2. XRD patterns using Co Kα radiation for (Ce,Gd)-Fe-B ribbons.

formation energy of $Ce_2Fe_{14}B$ crystal from those of other $R_2Fe_{14}B$ structure due to the lower solidus temperature of $Ce_2Fe_{14}B$ and the mixed valency of Ce [20,22]. For lower surface velocity of rotating copper wheel in rapid solidification the amount of amorphous phase should decrease and the intensity of diffraction peak may improve a little, but the coercivity decreased and the squareness of demagnetization curve deteriorated for $Ce_{13}Fe_{81}B_6$. It can be seen that Gd substitution leads to the increase in the intensity of diffraction peak, suggesting the reduction in the amount of amorphous phase and the improvement of the stability of $R_2Fe_{14}B$ structure. In addition, there still coexist the minor phase of RFe_2 in these ribbons in $Ce_{12}Gd_1Fe_{81}B_6$, $Ce_8Gd_5Fe_{81}B_6$, and $Gd_{13}Fe_{81}B_6$ ribbons. The diffraction peak of RFe_2 is much weaker in $Ce_{13}Fe_{81}B_6$, which should be attributed to the composition optimization for Ce content in Ce-Fe-B ternary alloys [19]. The lattice parameters were obtained by cell refinement using Jade software. Table 1 lists the lattice parameters of main phase $R_2Fe_{14}B$ and magnetic properties for (Ce,Gd)-Fe-B ribbons at temperature of 300 K. In $Ce_{13}Fe_{81}B_6$ ribbons the lattice constants a and c are 8.78 Å and 12.16 Å, respectively, much larger than the theoretical values, 8.76 Å and 12.11 Å [9]. The larger lattice parameters may ascribe to the defects and the imperfection of $Ce_2Fe_{14}B$ crystal, such as lattice distortion [23], which may result from the difficulty of the phase formation in rapid solidification. The distortion would reduce the magnetocrystalline anisotropy and therefore decrease the coercivity [24]. For Gd substitution, the lattice constant c decreases and is close to theoretical value.

The main phase for $R_2Fe_{14}B$ crystalline structure is ferromagnetic at room temperature. However, the structure is disordered in long-range for amorphous phase of Ce-Fe-B, which undergoes the magnetic phase transition from ferromagnetic to paramagnetic state near room temperature [21]. $CeFe_2$ phase is also paramagnetic state at room temperature [25,26]. The intergranular amorphous phase and minor phase isolate the nanostructure grains of ferromagnetic main phase, which may weaken the coupling among grains. Henkel plots are used to evaluate the intergranular exchange coupling effect and the uniformity of magnetization reversal among grains, which is defined as $\delta m = [2M_r(H) + M_d(H)]/M_r - 1$ [27,28]. Here $M_r(H)$ is the initial remanence obtained by the application and subsequent removal of a magnetic field H on the thermal demagnetization sample, M_r is the remanence, and $M_d(H)$ is the demagnetization remanence obtained by the application and subsequent removal of a negative field H for the sample magnetized to saturation in positive direction. Positive value of δm implies that exchange coupling is dominant over the dipolar interaction. Fig. 3 shows the δm curve for some $(Ce,Gd)_{13}Fe_{81}B_6$ ribbons, and the inset of Fig. 3 shows the variation of δm maximum with Gd atomic percent content. With the increase of Gd atomic percent, the maximum of δm increases

Table 1
Lattice parameters and magnetic properties for (Ce,Gd)-Fe-B ribbons.

Composition	Lattice constant a (Å)	Lattice constant c (Å)	H_c (kOe)	$(BH)_{max}$ (MGOe)	T_c (K)
$Ce_{13}Fe_{81}B_6$	8.78	12.16	4.43	7.31	442
$Ce_{12.8}Gd_{0.2}Fe_{81}B_6$	8.77	12.13	4.81	7.23	
$Ce_{12.2}Gd_{0.8}Fe_{81}B_6$	8.75	12.12	5.64	6.95	
$Ce_{12}Gd_1Fe_{81}B_6$	8.75	12.11	5.88	6.75	463
$Ce_8Gd_5Fe_{81}B_6$	8.76	12.10	5.40	5.36	545
$Gd_{13}Fe_{81}B_6$	8.77	12.10	3.19	2.92	609

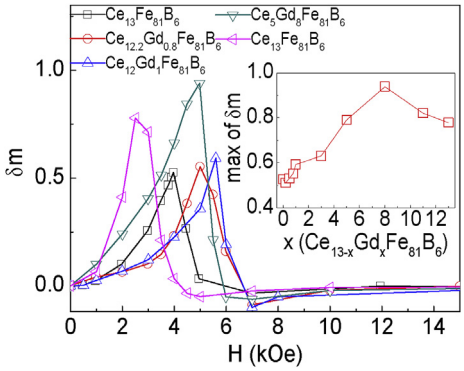

Fig. 3. δm curves for the samples at temperature of 300 K, and the inset shows the dependence of δm maximum on the Gd atomic percent.

and reaches to a peak in $Ce_8Gd_5Fe_{81}B_6$ ribbons, and then declines. A little amount substitution of Gd for Ce reduces the amount of amorphous phase, and so the magnetic isolating effect is weakened, giving rise to the enhancement of coupling effect and the increase of the maximum of δm. The squareness of demagnetization curve also improves in $Ce_5Gd_8Fe_{81}B_6$ ribbons, which should be related with the increase of δm maximum and result from the improvement in the uniformity of magnetization reversal [28].

For further checking the effect of Gd substitution for Ce on the magnetic properties, magnetization versus temperature was measured by the following method (shown in Fig. 4). The sample was magnetized to the saturation, and then set the applied field fixed at 1 kOe, increased temperature from 300 K and recorded the magnetization. The abrupt change of magnetization shown by the arrow corresponds to Curie temperature for the phase transition from ferromagnetic to paramagnetic state. Curie temperature is 442 K for $Ce_{13}Fe_{81}B_6$ ribbons, and Gd substitution leads to an increase of Curie temperature, indicating the increase of exchange coefficient between atoms in the main phase of $R_2Fe_{14}B$ [19]. This is the reason why the thermal stability is improved for Gd

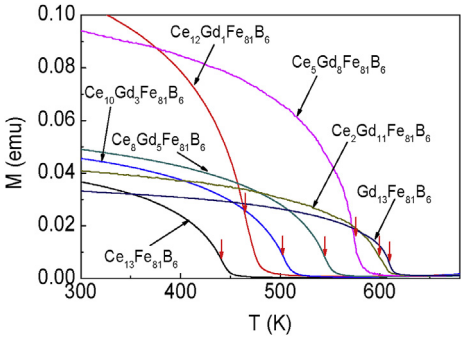

Fig. 4. Magnetization variations with temperature under the field of 1 kOe for the (Ce,Gd)-Fe-B ribbons.

substitution [29]. The increase of exchange coefficient would be beneficial to the enhancement of exchange coupling effect. So the increase of δm maximum originates not only from the decrease in the amount of amorphous phases, but from the increase of exchange coefficient in the main phase of $R_2Fe_{14}B$. For $Ce_2Gd_{11}Fe_{81}B_6$ and $Gd_{13}Fe_{81}B_6$ ribbons, the decrease of δm maximum may mainly result from the combined effect of the weak magnetocrystalline anisotropy and the dipole interaction. For isotropic nanocrystalline magnets magnetization reversal occurs firstly in the grains with low effective anisotropy, in which the anisotropy energy as well as the exchange energy is overcome by the applied field with the assist of dipolar interaction [30,31]. For high anisotropy and high applied field in high coercivity magnets, the effect of dipole interaction is weak and negligible [31]. As the anisotropy becomes weak, the dipolar interaction can't be neglected, which promotes the magnetization reversal firstly in the lower effective anisotropy grains, leading to the non-uniform magnetization reversal and the decrease of δm maximum.

4. Conclusions

In summary, the phase constitution and magnetic properties were investigated in $Ce_{13-x}Gd_xFe_{81}B_6$ ($x = 0–13$) ribbons by varying the relative content of Ce and Gd. The abnormal increase of lattice constants may result in the decrease of coercivity in $Ce_{13}Fe_{81}B_6$ ribbons. A little amount of Gd substitution for Ce improves the stability of $R_2Fe_{14}B$ phase and reduces the amount of amorphous phase, and the lattice constant c decreases. The coercivity increases for $x \leq 1$, but decreases for $x \geq 3$ in $Ce_{13-x}Gd_xFe_{81}B_6$. Curie temperature increases due to the Gd substitution for Ce, and the intergranular exchange coupling effect strengthens ascribing to the reduction in the amount of amorphous phase and the increase of exchange coefficient. It is expected that these investigations could serve as a reference for the chemical component design on the resource-saving Ce-based rare-earth magnets.

Acknowledgements

The present work was supported by the National Natural Science Foundation of China (Grant No. 51461033, and 51590880), the National Basic Research Program of China (Grant No. 2014CB643702) and the National Key Research and Development Program of China (No. 2016YFB0700900).

References

[1] A.K. Pathak, K.A. Gschneidner Jr., M. Khan, R.W. McCallum, V.K. Pecharsky, J. Alloys Compd. 668 (2016) 80.
[2] M.G. Zhu, W. Li, J.D. Wang, L.Y. Zheng, Y.F. Li, K. Zhang, H.B. Feng, T. Liu, IEEE Trans. Magn. 50 (2014) 1000104.
[3] E.J. Skoug, M.S. Meyer, F.E. Pinkerton, M.M. Tessema, D. Haddad, J.F. Herbst, J. Alloys Compd. 574 (2013) 552.
[4] J. Jin, Y. Zhang, G. Bai, Z. Qian, C. Wu, T. Ma, B. Shen, M. Yan, Sci. Rep. 6 (2016) 30194.
[5] A.M. Gabay, A. Martín-Cid, J.M. Barandiaran, D. Salazar, G.C. Hadjipanayis, AIP Adv. 6 (2016) 056015.
[6] K. Pei, X. Zhang, M. Lin, A. Yan, J. Magn. Magn Mater. 398 (2016) 96.

[7] B.J. Ni, H. Xu, X.H. Tan, X.L. Hou, J. Magn. Magn Mater. 401 (2016) 784.
[8] M. Hussain, L.Z. Zhao, C. Zhang, D.L. Jiao, X.C. Zhong, Z.W. Liu, Phys. B 483 (2016) 69.
[9] J.F. Herbst, Rev. Mod. Phys. 63 (1991) 819.
[10] J.M.D. Coey, Scr. Mater. 67 (2012) 524.
[11] J.Y. Jin, T.Y. Ma, Y.J. Zhang, G.H. Bai, M. Yan, Sci. Rep. 6 (2016) 32200.
[12] E. Isotahdon, E.H. Saarivirta, V.T. Kuokkala, J. Alloys Compd. 692 (2017) 190.
[13] B.X. Peng, T.Y. Ma, Y.J. Zhang, J.Y. Jin, M. Yan, Scr. Mater. 131 (2017) 11.
[14] A.K. Pathak, M. Khan, K.A. Gschneidner Jr., R.W. McCallum, L. Zhou, K. Sun, M.J. Kramer, V.K. Pecharsky, Acta Mater. 103 (2016) 211.
[15] W. Cui, T. Zhang, X. Zhou, D. Yu, Q. Wang, X. Zhao, W. Liu, Z. Zhang, Mater. Lett. 191 (2017) 210.
[16] X.B. Liu, Z. Altounian, M. Huang, Q. Zhang, J.P. Liu, J. Alloys Compd. 549 (2013) 366.
[17] J.F. Herbst, M.S. Meyer, F.E. Pinkerton, J. Appl. Phys. 111 (2012) 07A718.
[18] C.J. Yan, S. Guo, R.J. Chen, D. Lee, A.R. Yan, Chin. Phys. B 23 (2014) 107501.
[19] Z.B. Li, M. Zhang, B.G. Shen, F.X. Hu, J.R. Sun, Mater. Lett. 172 (2016) 102.
[20] C.J. Yan, S. Guo, R.J. Chen, D. Lee, A.R. Yan, IEEE Trans. Magn. 50 (2014) 2104604.
[21] Z.B. Li, L.L. Zhang, X.F. Zhang, Y.F. Li, Q. Zhao, T.Y. Zhao, B.G. Shen, J. Phys. D Appl. Phys. 50 (2017) 015002.
[22] A. Alam, D.D. Johnson, Phys. Rev. B 89 (2014) 235126.
[23] D.P. Kozlenko, K. Drużbicki, S.E. Kichanov, E.V. Lukin, H.P. Liermann, K.V. Glazyrin, B.N. Savenko, Phys. Rev. B 95 (2017) 054115.
[24] G. Hrkac, T.G. Woodcock, C. Freeman, A. Goncharov, J. Dean, T. Schrefl, O. Gutfleisch, Appl. Phys. Lett. 97 (2010) 232511.
[25] T. Nakama, K. Uchima, M. Hedo, T. Fujiwara, H. Fujii, A.T. Burkov, K. Yagasaki, J. Magn. Magn Mater. 272 (2004) 485.
[26] M. Zhang, Z.B. Li, B.G. Shen, F.X. Hu, J.R. Sun, J. Alloys Compd. 651 (2015) 144.
[27] P.E. Kelly, K. O'Grady, P.I. Mayo, R.W. Chantrell, IEEE Trans. Magn. 25 (1989) 3881.
[28] Z.B. Li, M. Zhang, B.G. Shen, J.R. Sun, Appl. Phys. Lett. 102 (2013) 102405.
[29] D.N. Brown, D. Lau, Z. Chen, AIP Adv. 6 (2016) 056019.
[30] R. Fischer, H. Kronmüller, J. Magn. Magn Mater. 191 (1999) 225.
[31] H.W. Zhang, C.B. Rong, X.B. Du, S.Y. Zhang, B.G. Shen, J. Magn. Magn Mater. 278 (2004) 127.